The crystal structure of recombinant rat pancreatic RNase A

ARTICLE *in* PROTEINS STRUCTURE FUNCTION AND BIOINFORMATICS · APRIL 1999

Impact Factor: 2.63 · DOI: 10.1002/(SICI)1097-0134(19990401)35:1<1::AID-PROT1>3.0.CO;2-2

RESEARCH ARTICLES

The Crystal Structure of Recombinant Rat Pancreatic RNase A

V. Gupta,[1] S. Muyldermans,[2] L. Wyns,[2] and D.M. Salunke[1]*
[1]*Structural Biology Unit, National Institute of Immunology, New Delhi, India*
[2]*Institute of Molecular Biology, Vrije University of Brussels, Brussels, Belgium*

ABSTRACT **The three-dimensional structure of rat pancreatic RNase A expressed in *Escherichia coli* was determined. The backbone conformations of certain critical loops are significantly different in this enzyme compared to its bovine counterpart. However, the core structure of rat RNase A is similar to that of the other members of the pancreatic ribonuclease family. The structural variations within a loop bordering the active site can be correlated with the subtle differences in the enzymatic activities of bovine and rat ribonucleases for different substrates. The most significant difference in the backbone conformation was observed in the loop 15–25. This loop incorporates the subtilisin cleavage site which is responsible for RNase A to RNase S conversion in the bovine enzyme. The rat enzyme does not get cleaved under identical conditions. Molecular docking of this region of the rat enzyme in the active site of subtilisin shows steric incompatibility, although the bovine pancreatic ribonuclease A appropriately fits into this active site. It is therefore inferred that the local conformation of the substrate governs the specificity of subtilisin. Proteins 1999;35:1–12.** © **1999 Wiley-Liss, Inc.**

Key words: subtilisin-resistant RNase A; substrate specificity; molecular docking; active site geometry; homologous enzymes

INTRODUCTION

Ribonucleases of the bovine pancreatic superfamily have played a critical role in establishing the protein structural correlations with their biochemical properties.[1–5] Detailed structural investigations have been carried out on several ribonucleases by application of X-ray and neutron diffraction techniques. These include, for example, bovine pancreatic[6–8] and seminal ribonucleases,[9] the human angiogenin[10] and the ribonuclease from *Rana pipiens* oocyte.[11] Proteins from closely related species with shared function constitute a family with naturally engineered modifications where certain optimization has evolved through successive mutations. The comparative analysis of such protein families enables understanding the finer aspects of structure, folding and mechanism of action.

The pancreatic ribonucleases also provide an appropriate model for understanding the molecular determinants of substrate recognition by subtilisin, a bacterial serine protease. Many of the ribonucleases get cleaved at a specific site when subjected to limited proteolysis by subtilisin without significantly affecting the three-dimensional structure or the enzymatic activity. This property has been exploited while designing experiments to probe protein structure and folding.[12,13] Certain members of this superfamily, which include rat pancreatic RNase A, are known to resist this cleavage by subtilisin.[14] The structure of rat RNase A and its comparison with the bovine RNase A reported in this paper provide an insight into the structural aspects of the substrate specificity of subtilisin. Also, the structure of rat RNase A has wider implications for understanding the amino acid substitutions in homologous proteins with reference to structural stability and functional constraints.

MATERIALS AND METHODS

Preparation of Recombinant Rat RNase A

All DNA manipulations were carried out by standard procedures as described by Sambrook et al.[15] Rat pancreatic RNase A was cloned in the expression vector pMa5–8[16] under the control of an IPTG (Boehringer, Mannheim) inducible P_{tac} promoter and phoA signal region to direct the protein to the periplasm of *E. coli* strain JM101. While cloning, the first three amino acids were deleted and the fourth residue, Arg, was mutated to Ala for successful expression of the protein in the periplasmic region of *E. coli*.

Abbreviations: RNase A, ribonuclease A; 2′3′-CMP, Cytidine 2′:3′-cyclic monophosphate; 2′3′-UMP, Uridine 2′:3′-cyclic monophosphate; RNA, ribonucleic acid; LB, luria-bertani medium; TB, terrific broth; PEG, polyethyleneglycol; Single letter codes for amino acid residues with residue number preceding the name and r or b abbreviated for rat and bovine, respectively.

Atomic coordinates have been deposited with the Protein Data Bank, Brookhaven National Laboratory.

*Correspondence to: Dinakar M. Salunke, Structural Biology Unit, National Institute of Immunology, Aruna Asaf Ali Marg, New Delhi 110 067, India. E-mail: dinakar@nii.ernet.in

Received 14 July 1998; Accepted 23 November 1998

The periplasmic protein was released by osmotic shock procedure as described by Neu and Heppel.[17] Briefly, the procedure involved suspending the cell pellet from an overnight culture in 20% sucrose; 0.05M Tris (pH 7.5); 0.01 M EDTA; 0.02 mM PMSF, followed by 30 min incubation on ice. The suspension was centrifuged (30 min at 8,000 rpm in GS-3 rotor at 4°C) and the pellet was subjected to osmotic shock by adding an equal volume of ice cold water and mixing thoroughly. The suspension was again incubated on ice for 30 min, centrifuged (8,000 rpm, 30 min, GS-3 rotor) at 4°C and the supernatant removed. Most (60%–70%) of the ribonuclease was released during treatment with sucrose solution and the remaining protein was set free on stirring with cold water. Both fractions were loaded separately onto a CM C-25 sephadex cation exchanger (Pharmacia) after 2-fold dilution with the column running buffer (10 mM Tris; 1 mM EDTA; 0.02 mM PMSF; pH 7.5). Proteins were eluted with a 0.05–0.5 M NaCl gradient. The fractions containing RNase A were pooled and dialyzed against water. Lyophilized RNase A was stored at 4°C. Purity of the protein was confirmed by SDS-PAGE and N-terminal sequencing.

RNase Activity Assay

RNA-agar plate assay

A solution containing 2% (w/v) agar (Bacto-agar), 0.3% (w/v) Yeast Torula RNA (Sigma) in 0.1 M Tris-HCl, pH 7.5 was autoclaved and spread in petri dishes. Round holes were made in the RNA agar and recombinant or commercial bovine RNase A (Boehringer Mannheim) was applied in a volume of 10 µl. The plates were incubated for 1–2 h at 37°C. To visualize RNase activity, 2 N HCl was poured over the plate. A clear halo is produced for hydrolyzed RNA, whereas, the RNA that has not been hydrolyzed forms a cloudy precipitate.

Spectrophotometric assay

Reactions were performed in 0.2 M Tris-HCl; 0.02 M EDTA; pH 7.5 using a quartz cuvette of 1.0 cm optical path length. The activities of both bovine as well as recombinant rat ribonuclease on 0.1% 2′3′-CMP and 0.1% 2′3′-UMP were measured as per Crook et al[18] by following the rise in absorbance at 284 nm and 274 nm, respectively for the two cyclic substrates. Yeast Torula RNA at a concentration of 0.05% was used as substrate and the absorbance change was monitored at 298.5 nm.

Crystallization and Data Collection

The enzyme was crystallized using vapor diffusion in hanging drops. Crystallization experiments were set up using various combinations of reagents and buffers in Linbro 24-well tissue-culture plates (Nunc, Denmark). Polyethylene glycols of different molecular weights (Sigma Chemical Company), ammonium sulfate, sodium sulfate and 2-methylpentan-2,4-diol were used as precipitants. Hanging drops of 10 µl volume containing 5 µl protein solution and 5 µl precipitant were set up in the tissue culture plates covered by siliconized cover slips.

The X-ray intensity data were collected on 300 mm Image Plate detector (Marresearch, Norderstedt, Germany) at NII, New Delhi, installed on a rotating anode X-ray source (RIGAKU) operated at 40 kV and 70 mA (CuK radiation) with a Ni monochromator and a 0.5 mm collimator. Intensity data were processed with the DENZO[19] suite of programs.

Structure Determination and Refinement

All molecular replacement calculations were carried out using the program AMoRe.[20] The cross-rotation function, translation function and rigid body refinement calculations were carried out using ROTING, TRAING, and FITTING modules in AMoRe, respectively. Bovine RNase A (pdb7rsa)[21] was selected from the PDB[22] and used as a probe model for rotation/translation function calculations. A triclinic artificial unit cell with each dimension equal to 100 Å and a radius of integration of 14 Å was used for these calculations. After applying the rotation-translation solution to the model it was subsequently subjected to rigid body refinement in X-PLOR[23] which was followed by conventional energy minimization (Powell method) combined with simulated annealing. The molecule was heated from 300 K to 3,000 K for simulated annealing in X-PLOR. The refinement carried out using all data in the resolution range of 8 to 2.5Å gave a conventional crystallographic R factor of 18.6% and a free R of 27.7%. Electron density maps were displayed using the program O[24] on an INDIGO[2] (Silicon Graphics Inc.). Manual rebuilding of the intermediate models was performed using the program O based on various 2Fo-Fc and Fo-Fc electron density maps. The correspondence between the polypeptide chain and the electron density map is good in most parts of the map and the backbone structure of RNase A closely resembles that observed in bovine RNase A.

RESULTS AND DISCUSSION

Recombinant Rat RNase A

Rat RNase A has been expressed in *E. coli* under the control of P_{tac} promoter and phoA signal for directing the protein to periplasmic space. The expressed protein is a mutant (Fig. 1A) in which the first three amino acids were deleted as they are absent in all the other homologous ribonucleases[25] and, therefore, not considered necessary for ribonuclease activity. The fourth amino acid was mutated from Arg to Ala for proper cleavage of the signal sequence.[26] The level of production of the enzyme in JM101 cells is 5 mg/l culture. Overproduction of RNase A can be readily visualized by fractionation of cellular extracts on SDS polyacrylamide gel (Fig. 2). RNase A sequestered in the periplasmic space was released by osmotic shock and was purified by one step column chromatography. Both sucrose and cold water fractions (see experimental procedures) were separately subjected to chromatography on the CM-sephadex C-25 column which yielded 3–4 mg/l and 1–2 mg/l of pure recombinant RNase A, respectively. The cation-exchange column was found to be appropriate due to the basic character of the protein. Since most of the *E. coli* periplasmic proteins are acidic in nature, one

A

```
                1                   20                  40
                |                   |                   |
Bovine      ---KETAAAKFERQHMDSSTSAASSSNYCNQMMKSRNLTKDRCKPVNTFV
r. Rat      ---AESSADKFKRQHMDTEGPSKSSPTYCNQMMKRQGMTKGSCKPVNTFV
w. Rat      GESRESSADKFKRQHMDTEGPSKSSPTYCNQMMKRQGMTKGSCKPVNTFV
               *  * ** *****      **  *******    **  ********

                        60                  80
                        |                   |
Bovine      HESLADVQAVCSQKNVACKNGQTNCYQSYSTMSITDCRETGSSKYPNCAY
r. Rat      HEPLEDVQAICSQGQVTCKNGRNNCHKSSSTLRITDCRLKGSSKYPNCDY
w. Rat      HEPLEDVQAICSQGQVTCKNGRNNCHKSSSTLRITDCRLKGSSKYPNCDY
            ** * **** ***  * ****  **  * **  *****  ******** *

              100                 120
              |                   |
Bovine      KTTQANKHIIVACEGNPYVPVHFDASV
r. Rat      TTTDSQKHIIIACDGNPYVPVHFDASV
w. Rat      TTTDSQKHIIIACDGNPYVPVHFDASV
             **   **** ** *************
```

B

	15	*16*	*17*	*18*	*19*	*20*	*21*	*22*	*23*	*24*	*25*
Kangaroo	T	E	H		T						
Reindeer	P		P		S						
Red deer	P				S						
Giraffe					S	V					
Dromedary	Y	S		S	S		N				
Bovine	**S**	**S**	**T**	**S**	**A**	**A**	**S**	**S**	**S**	**N**	**Y**
Rat	T	E	G	P	S	K			P	T	
Bovine seminal plasma	G	N		P	S						
Pig	P	D	S		S	S	N				
Coypu	R	G		P	S	T	N	P			
Lesser rorqual	G	N		P	G	N	N	P			

Fig. 1. **(A)** The comparison of sequences of the bovine, the wild type rat (w. rat) as well as the genetically engineered rat (r. rat) RNase A. The numbering is with respect to the bovine sequence and the identical residues in the three sequences are indicated by '*'. **(B)** The comparison of the sequence segments corresponding to the subtilisin cleavage site (residues 15–25) in the pancreatic RNases from different species. The residues which are different from those of bovine RNase A have been indicated for the enzymes from other species. The residues above the rat sequence are cleaved by subtilisin while the rat and the ones below it are not cleaved.

step column chromatography yields pure protein. The N-terminal sequencing of the first 20 residues on an automatic protein sequencer ABI470 established not only that the protein is pure but also that it is the desired one.

Ribonuclease activity of the recombinant rat RNase A was compared with the bovine RNase A using different substrates. At pH 7.5, the activity of the recombinant rat enzyme on ribonucleic acid (Fig. 3A) and cytidine 2′:3′-cyclic monophosphate (Fig. 3B) is less than that of the bovine enzyme. On the other hand, the rat enzyme shows significantly higher activity on uridine 2′:3′-cyclic monophosphate (Fig. 3C) as compared to that of the bovine enzyme. The comparison of the activity of purified wild type rat ribonuclease A with the bovine enzyme[27] also shows similar profiles as our recombinant enzyme, implying that the N-terminal residues which have been mutated are not involved in the activity.

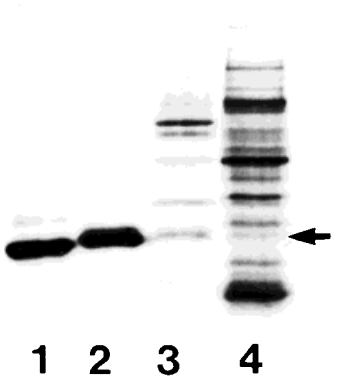

Fig. 2. SDS-PAGE of fractionation of cellular extracts of recombinant rat RNase A during purification. Lane 1 corresponds to the commercially obtained bovine RNase A. The lanes 2–4 corresponds to the CM-sephadex purified recombinant rat ribonuclease A, sucrose fraction and the aqueous fraction obtained during purification. The band corresponding to the recombinant rat RNase A is marked by an arrow.

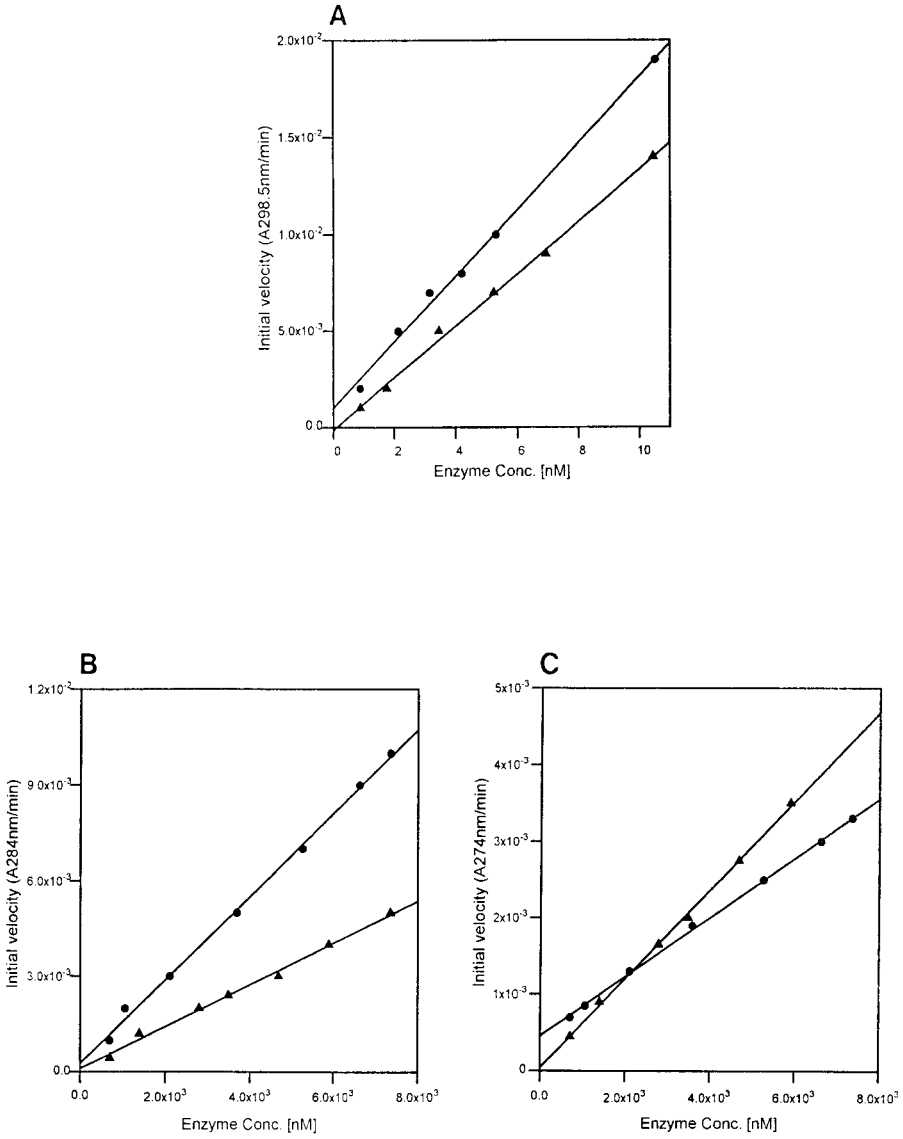

Fig. 3. The comparison of the enzymatic activities of the genetically engineered rat (▲) and bovine RNase A (●) at pH 7.5 against **(A)** Yeast torula RNA, **(B)** 2′3′-CMP, and **(C)** 2′3′-UMP. Average standard error on initial velocity is about 5×10^{-4}.

Crystallization and Data Collection

The crystals of recombinant RNase A were obtained using a starting protein concentration of 20 mg/ml from the solution of 10 mM acetate buffer containing 1 mM disodium hydrogen phosphate at pH 5.3 after equilibrating with 35% polyethylene glycol (molecular weight 8,000 Da). The choice of the bacterial growth medium appears to have been very critical for the protein crystallization. The protein extracted from the cells did not crystallize if the growth medium for bacterial cells was changed from TB to LB. Excessive phosphate content of TB medium[28] compared to that of the LB medium[15] may be relevant here since RNase A is generally known to crystallize with bound phosphate/sulphate ligand.

The crystals diffracted up to 2.5 Å resolution and were suitable for structural studies. The intensity data were collected on an image plate at a crystal to detector distance of 90 mm by recording 1° frames using a single crystal. The crystal was mounted in a random orientation and 66 frames were collected. The final data set had 4,534 unique reflections representing 80% completeness at 2.5 Å resolution with a $R_{merge} = 10.6\%$. The crystals lasted for about 40 h in the X-ray beam which was adequate for intensity data collection using one single crystal. The crystals belong to the space group $P3_121$ with unit cell dimensions of $a = 69.1$ Å and $c = 60.9$ Å. The space group ambiguity with regard to the enantiomorph was resolved by comparing the translation function solution in both, $P3_121$ and $P3_221$,

TABLE I. Preliminary Characterization and Statistics of Data

Space group	$P3_121$
Unit cell dimensions	a = 69.13 Å
	b = 69.13 Å
	c = 60.93 Å
Solvent content	59.9%
Molecules in unit cell (Z)	6
Matthews constant (V_m)	3.07 Å^3/Da
Data collection statistics	
Resolution of data	2.5 Å
Number of reflections	4534
R_{merge}	10.6%
Redundancy	2.9
Data statistics for the last resolution bin (2.75–2.5 Å)	
Completeness	60%
R_{merge}	15.6%
Average I/σ_1	1.9

space groups. Since the molecular weight of RNase A is 13,600 Da, the Matthews Constant (V_m)[29] of the crystals is 3.07 Å^3/Da. This suggests the presence of 1 molecule in the asymmetric unit with solvent content of about 62%. The crystal data and the intensity statistics are listed in Table I.

Structure Determination and Refinement

Molecular replacement was the obvious choice for determination of the recombinant rat RNase A structure since it has about 68% sequence identity with bovine RNase A, a protein for which a refined high resolution structure is available. Among the different crystal structures available for RNase A, phosphate free bovine pancreatic RNase A refined at 1.26 Å resolution[21] appeared to be a suitable model. The molecular replacement calculations were performed with this model (pdb code: 7rsa), a polyalanine model corresponding to the 7rsa template (7rsa_ala) as well as a model (7rsa_rat) generated by substituting alanine in 7rsa structure for those residues that differ between bovine and rat RNase A. All these models gave a common solution. However, the 7rsa_rat was significantly superior in terms of the correlation coefficient and R-factor. Therefore, subsequent refinement was carried out using this model. The summary of the molecular replacement parameters using this data is given in Table II. The highest peak at 22.9σ corresponded to the correct solution, whereas the next peak was at 18.4σ.

The properly oriented and positioned 7rsa_rat was transferred to the program X-PLOR for further refinement. Both conventional R_{cryst} and R_{free} (values 5% of total reflections) were used to monitor the refinement progress. The initial model was subjected to rigid body refinement between 10 to 4 Å which gave R_{free} and R_{cryst} of 41.1% and 40.2%, respectively. Subsequent refinement included several rounds of simulated annealing and positional refinement with appropriate weighting between the diffraction data and stereochemical restraints. Refinement was alternated with manual model revisions using the program O. Higher resolution diffraction data, up to 2.5 Å were added in a stepwise fashion as more substitutions were made and the intermediate structure converged. At this stage, the R_{free} and R_{cryst} were 34.3% and 24.2%, respectively. The model was subjected to 20 cycles of overall temperature factor and 20 cycles of individual temperature factors refinement. The results of the temperature factor refinement were evaluated by monitoring the changes in R_{cryst} and R_{free}. Both values improved by about 1% after temperature refinement (R_{free} and R_{cryst} were 33.0% and 22.9%, respectively). Water molecules were placed in sites which had difference density that was larger than 3σ in the Fo-Fc map, and showed a reasonable hydrogen bonding geometry. Water molecules with high temperature factors were retained if they showed difference electron density more than 2σ and appropriate hydrogen bonding environment. Regions with poor electron density were deleted from the model and rebuilt after refinement.

The initial electron density map of the structure showed reasonable fit for most of the backbone model derived from the 7rsa template except for the loop region around residue 20. Therefore, the residues 15–25 were deleted from the model and rebuilt manually with iterative refinement cycles. The rebuilding entailed shifting positions of the atoms by up to a maximum of 4.5 Å after which the loop fitted the electron density appropriately. The results of the final refinement using all data from 8.0 to 2.5 Å are summarized in Table III. No significant peaks were detected in the Fo-Fc difference density map corresponding to the final structure. The mean error of the coordinates is 0.25 Å as estimated by the method of Luzatti.[30] During the refinement 92 water sites were identified and included in the structure.

Overall Structure

The core structure of rat RNase A is very similar to that of the bovine RNase A. There are three helical segments corresponding to residues 3–13; residues 24–33; and residues 50–60. A large stretch of a curved antiparallel β-sheet exists incorporating residues 41–48, 71–92 and 94–110 with loops of various sizes separating different strands. The ribbon drawing representing the polypeptide chain fold is shown in Figure 4A. The final model of rat RNase A includes 958 protein atoms, 5 phosphate atoms, and 92 atoms corresponding to water molecules. The ϕ-ψ plot for backbone torsion angles is presented in Figure 4B. All the non-glycine residues are within the allowed regions of the ϕ-ψ plot. Among the seven prolines present, two (93P and 114P) are in the "*cis*" conformation while the others are in the "*trans*" conformation. Both the "*cis*" prolines are involved in sharp turns between β regions, and they are well-defined in both 2Fo-Fc and omit maps. The mean temperature factors of the main chain and side chains are plotted in Figure 5. Except for the stretch 15–25, the B values for the rest of the main chain atoms fall within 15–30 Å^2. The β values for this stretch are between 28–55 Å^2 indicating a higher flexibility of this loop in the molecule.

The rat RNase A structure shows significant local conformational differences in certain loop regions with respect to

TABLE II. Molecular Replacement Solution Using AMoRe

AMoRe	Resolution range (Å)	Rotation α	Rotation β	Rotation γ	Translation Δx	Translation Δy	Translation Δz	σ/C_f	R (%)
Roting	8–3	6.95	120.16	16.72				22.9	
Traing	8–4	6.95	120.16	16.72	0.561	0.764	0.092	50.8	42.2
Fitting	8–4	9.57	120.37	17.95	0.564	0.768	0.091	55.9	39.8

TABLE III. Refinement and Geometry Statistics

Resolution range	8–2.5 Å
Initial model	pdb7rsa
R_{cryst}	18.6%
R_{free}	27.7%
Number of protein atoms	951
Number of solvent atoms	92
Deviations from ideality	
r.m.s. bond lengths (Å)	0.012
r.m.s. bond angles (°)	1.96
r.m.s. dihedrals (°)	26.18
r.m.s. impropers (°)	1.68
Overall expected error in coordinates (Å)	0.25
Distribution of non-glycine, non-proline ϕ-φ angles in Ramachandran Plot	84% in most favored, 14% in additionally allowed and 2% in generously allowed regions

those of the bovine enzyme. The root mean square (RMS) difference between all the backbone atoms of bovine RNase A and of rat RNase A is 1.0 Å. Four loops, namely, 15–25, 59–62, 65–72 and 88–94 exhibit differences exceeding the overall RMS deviation with respect to the bovine enzyme by 4.3, 1.6, 2.3 and 1.4 Å, respectively. These regions are also highly variable in other RNase A structures. The RMS deviation between the backbone atoms excluding the four loops is 0.64 Å, indicating that the rest of the backbone structure is practically identical in the two proteins. The RMS deviation for the loops 59–62 and 88–94 could still be considered negligible. However, the two loops 15–25 and 65–72 differ significantly and this difference can be correlated directly with the biochemical properties associated with RNase A. The conformation of the loop 15–25 which connects the first and the second α-helix in bovine as well as in the rat enzymes is so different that the residues within this region had to be rebuilt in rat RNase A map. This region exhibits maximum backbone conformational difference between the two proteins. Although this loop does not have any direct involvement in the active site geometry, it is relevant for the RNase A to RNase S conversion. The other loop, 65–72, which is located on the periphery of the active site moves by about 2.3 Å and this change appears to modulate the activity of the enzyme.

There are 42 residues that are different between recombinant rat RNase A and bovine RNase A. Most of the differences are pair-wise, mutually complementing, if the residues have interactions between themselves. Some of the charge differences can be grouped into pairs, where the side chains of residues with opposite polarity of a pair approach each other closely in the three-dimensional structure of the enzyme. For instance, r87K-r96D form a salt bridge in the rat structure; both these residues (T and A, respectively) are uncharged in the bovine enzyme and are not involved in any significant mutual interaction. Similarly, the salt bridge r80R-r101D is a hydrogen-bonded interaction (b80S-b101Q) in bovine. The residues corresponding to two other such salt bridge interactions in rat enzyme (r6D–r9K and r69R–r111D), do not exhibit any mutual interaction in bovine, since one residue of either pair (b6A–b9E and b69Q–b111E) is changed to a neutral residue. The residues with side chains interacting predominantly with the solvent, do not exhibit such pair-wise correlation.

There are three substitutions in the hydrophobic core of the molecule which are clustered together in both enzymes. Two internal isoleucines at positions 57 and 108 are valines in the bovine enzyme. It appears that there is a space adjustment between b57V and b79M by changing them to r57I and r79L, respectively. However, the additional methylene of isoleucine in rat at position 108 appears to be filling in for an internal cavity. Although not directly involved in defining the active site, the change of b4A to r4S influences the geometry of the active site by forming a hydrogen bond between r4S and r119H thereby pulling this residue into the B-conformation. This change makes space for the loop 65–72 to move inwards by about 2.3 Å (Fig. 6B). Many surface residues in the rat enzyme which are smaller in size compared to the corresponding residues of the bovine enzyme are apparently compensated for by bound water molecules. For example, r33Q and two water molecules, W170 and W228, displace the bulkier residue b33R; r34G and a water molecule W197 displace b34N; and r39S, W215 and W216 substitute b39R. Similarly, b61K accounts for r61G and W233; W234 and b76Y account for r76S and W212. The variations in the residues within the four loops which have different backbone conformations in the two proteins have relatively different environments and may be responsible for the conformational differences. The remaining substitutions mostly involve surface residues of the molecule.

Active Site Residues

The substrate binding site of RNase A is defined by three sequentially reoccuring sub-sites B, R, P for the pyrimidine base, ribose associated with the pyrimidine and phosphate binding site, respectively.[31] Considering the sub-sites for the nucleotides on either side of the scissile phosphodiester bond (B1, R1, P1 and B2, R2 and P2), the active site of RNase A is defined by the side chains of 7K, 10R, 12H, 41K, 43V, 44N, 45T, 66K, 69Q, 71N, 111E, 119H,

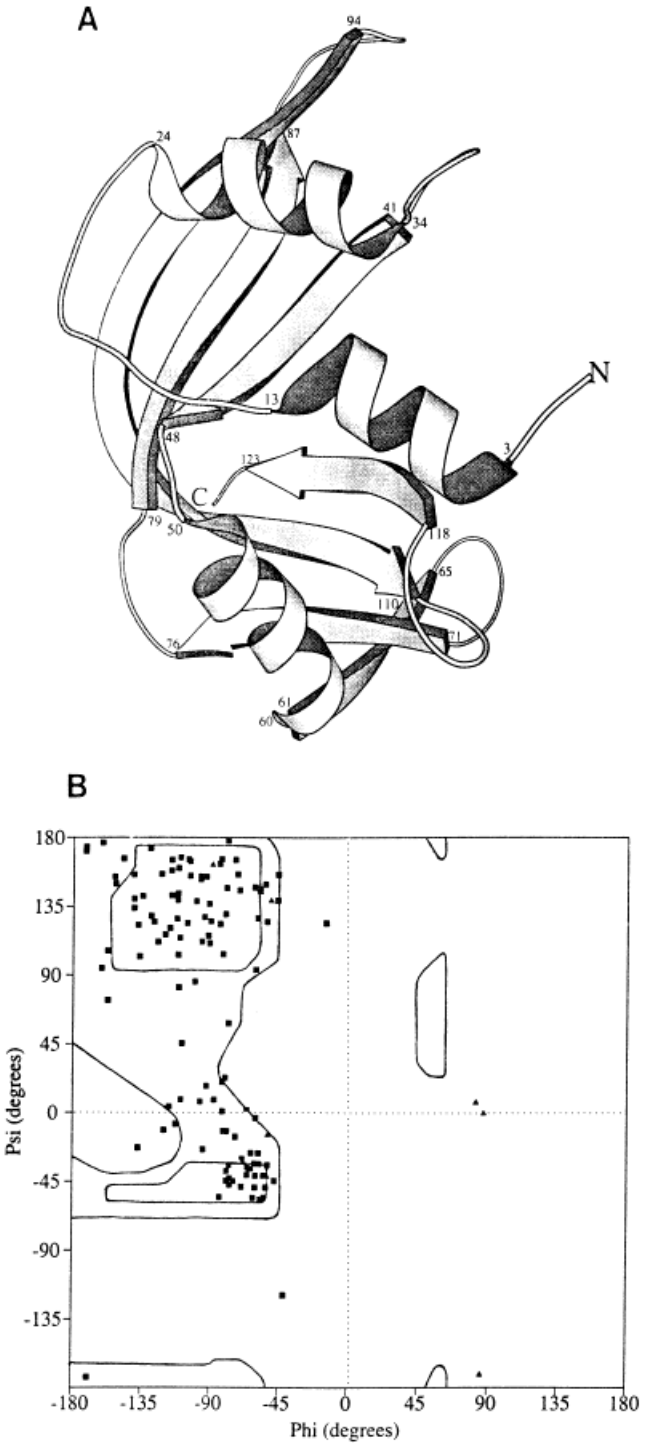

Fig. 4. **(A)** Ribbon drawing schematically showing the structure of the recombinant rat RNase A at 2.5 A resolution. The residues at the beginning and end of each secondary structural element have been numbered. **(B)** Ramachandran plot indicating the residues of the recombinant rat RNase A in allowed and disallowed regions.

120F, and 123S.[32] Among these, the residues 45T, 120F and 123S defining the B1 subsite and 41K, 119H, and 12H defining the P1 subsite are obviously the most critical as

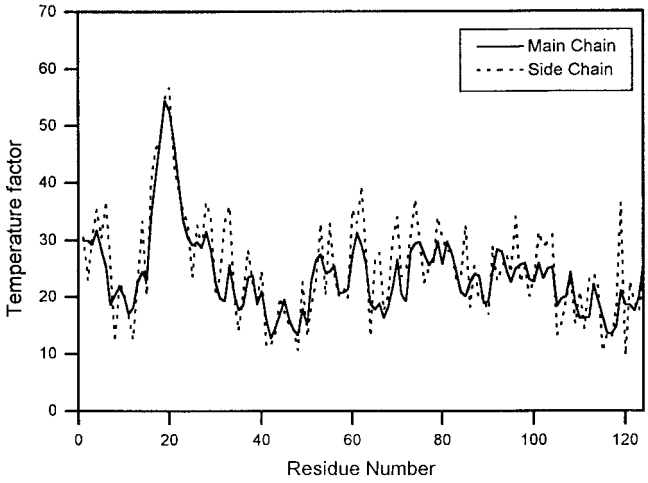

Fig. 5. Plot showing the average main chain and the side-chain temparature factors for all the residues of the recombinant rat RNase A.

they are in the close vicinity of the scissile phoshodiester bond. All these active site residues are conserved between the bovine and rat RNase A. However, the shape of the active site is not entirely identical in the two proteins (Fig. 6A).

Many differences between rat and bovine active site geometries are notable. In some of the previously described structures of bovine RNase A, b41K has been shown to be relatively flexible in certain cases, and to have high temperature factors in the absence of inhibitors.[31,33] In the present structure, 41K has relatively low temperature factors and clear electron density as is also the case with 7RSA and 1RPH. It does not interact with phosphate. The final refined model of 41K places the terminal nitrogen Nζ, 5.14 Å from the phosphorus and 4.34 Å from the O3 and 4.59 Å from the O4 oxygens of the phosphate. Nζ of 41K takes part in three hydrogen bonds, to 43V, 44N, and to one water molecule. 43V in bovine has no hydrogen bonds to either the protein molecule or to the solvent molecules, whereas in the rat enzyme the main chain is hydrogen-bonded to the protein molecule. The main chain atoms of 43V are stabilized by hydrogen bonds to water molecules and 41K. 12H is hydrogen-bonded to phosphate ion, one water molecule and main chain atoms of 8F and 45T. One phosphate ion is bound in the P1 site interacting with 12H, the backbone of 120F and three water molecules. The pyrimidine binding site B1 is occupied by a water molecule which mimics the base protein interaction by forming hydrogen bond with threonine Oγ1. It is known from the earlier studies on the X-ray structure of bovine RNase A that 119H can occupy two positions although various crystal structures show either one or the other position. Neutron diffraction studies[34] showed only the A conformation, whereas three other groups observed only the B conformation.[35–37] In inhibitor complexes of bovine RNase A, the situation seems to be slightly different, where, 119H always has a single conformation, which can either be the A[38–40] or the B conformation.[38] It appears that

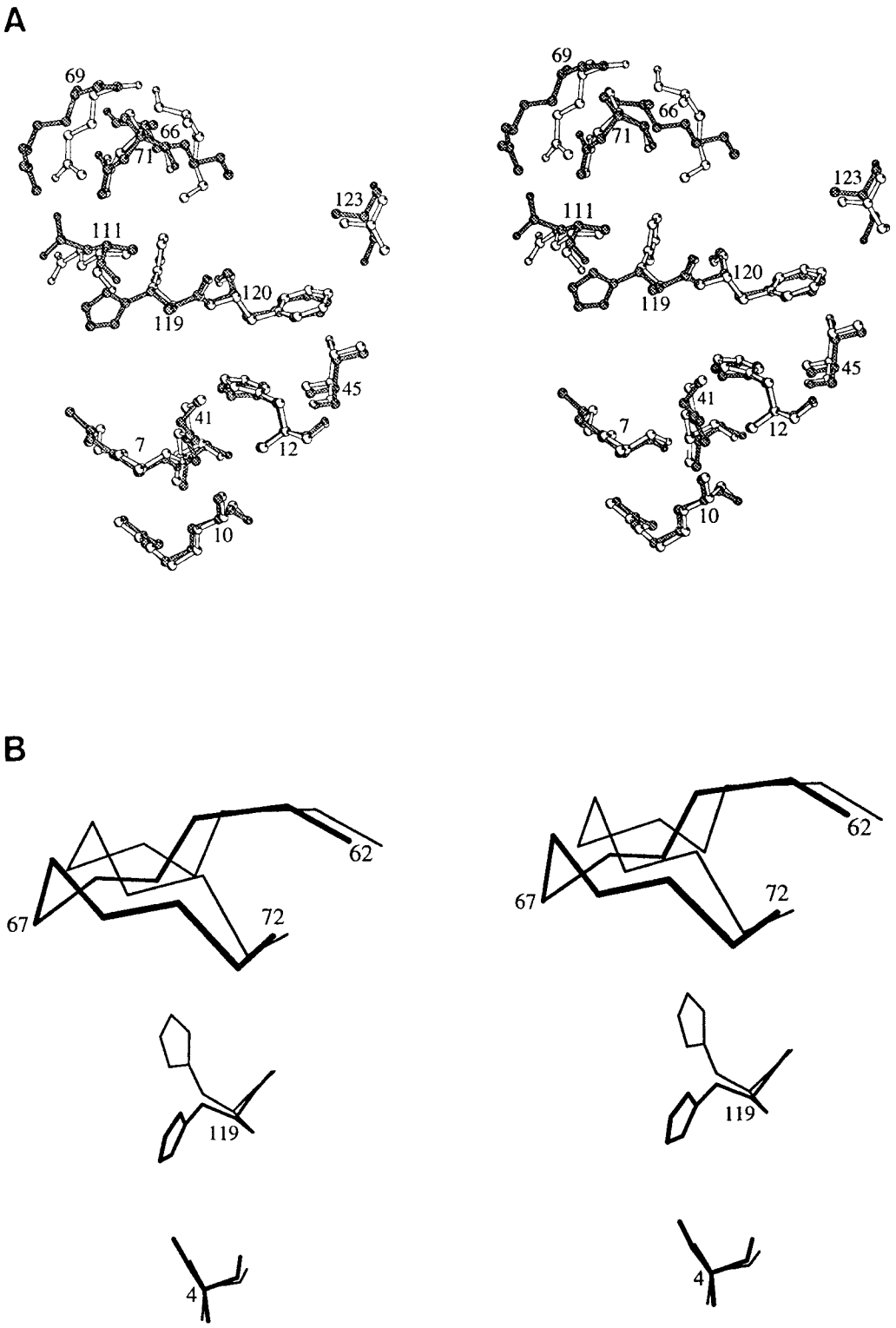

Fig. 6. Comparison of **(A)** active site geometry and **(B)** His119 geometry and its environment between rat (dark) and bovine (light) enzymes.

in the absence of a substrate or inhibitor, 119H is relatively mobile, and has two preferential conformations, A and B. In the present structure, however, 119H is less mobile and occupies the B conformation which is apparently stabilized by electrostatic interactions with 4S, unlike in case of bovine enzyme where it is alanine (Fig. 6). The Nε2 of

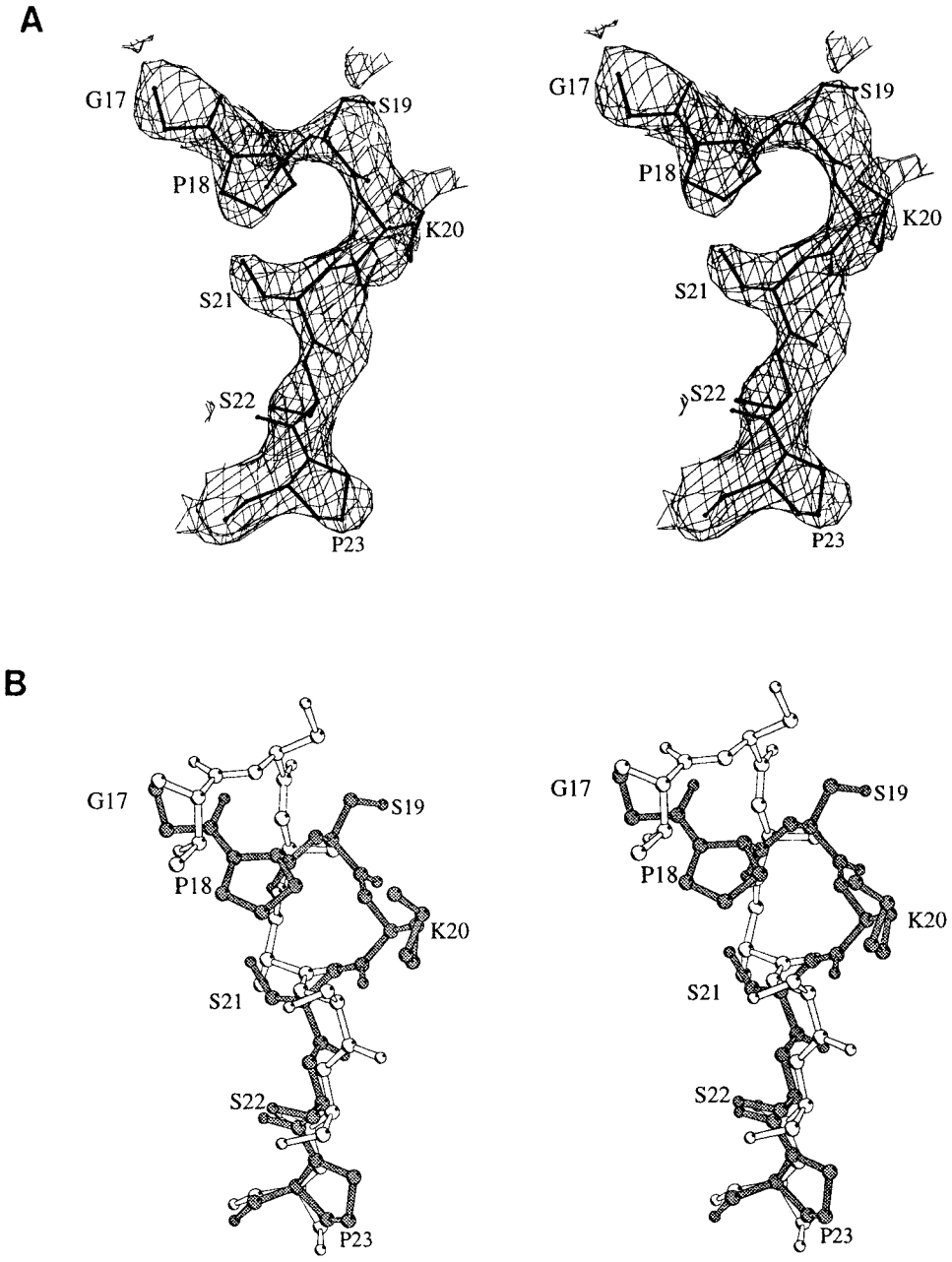

Fig. 7. Comparison of the subtilisin cleavage site of bovine RNase A with the corresponding loop of rat RNase A. **(A)** The stereoscopic drawing of the electron density map superimposed on the line drawing of the residues 17–23 of rat RNase A and **(B)** Stereoscopic drawings of the polypeptide chains corresponding to the residues 17–23 in rat (dark) and bovine (light) RNase A.

119H is within hydrogen-bonding distance (3.3 Å) from Oγ of 4S. It appears that the 4S is responsible for holding 119H in B conformation. Consequently, the loop 65–72 appears to be inwardly oriented with respect to the active site, by about 2.3 Å, directly affecting the subsites P0 and B2.[32] The inward orientation of this loop also makes the shape of the active site slightly smaller.

The changes in the shape of the active site in rat enzyme with respect to the bovine will naturally modulate the specificity of the enzyme against different substrates. In fact such a correlation is evident. The rat RNase A has comparatively lower activity against RNA (Fig. 3A). Although the B-conformation of 119H by itself should not be responsible for the reduced activity, the inward orientation of the loop 65–72 may be the reason for reduced affinity of the enzyme against the polymer substrate. There exists striking differences between the rat and bovine enzymes in their specific activity towards cyclic 2′,3′-CMP (Fig. 3B) and cyclic 2′,3′-UMP (Fig. 3C) as substrates. Binding of cytidine or uracil derivatives apparently affects the reactiv-

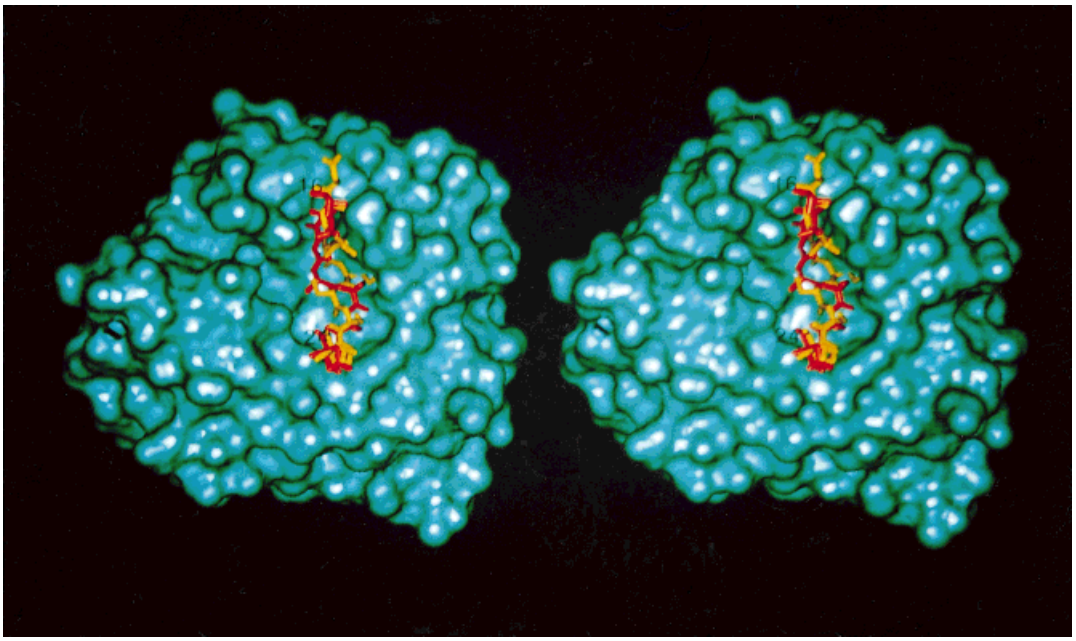

Fig. 8. Stereoscopic surface representation of subtilisin after molecular docking of the loop 16–24 of bovine (red) and rat (yellow) RNase A in it's active site.

ity of catalytic groups in the active site in both enzymes in a different manner.

Subtilisin Cleavage Site

Some enzymes have nearly absolute specificity for a given substrate and will not act on even very closely related molecules. On the other hand, certain enzymes have much broader specificity. One of the determinants providing this broad specificity is the adaptibility of the shape of the substrate-binding pocket through limited conformational flexibility in the active site. However, there are many enzymes that have an adequately well defined active site, yet they can work on a fairly broad range of substrates. Subtilisin is one such enzyme with an ill-defined substrate sequence signature. Subtilisin cleaves bovine RNase A between residues 20–21 when subjected to limited digestion,[41] breaking the protein into two covalent chains called S-peptide (residues 1–20) and S-protein (residues 21–124). In spite of this cleavage, RNase A still retains its complete enzymatic activity in the proteolytically processed enzyme, called RNase S. The S-peptide and the S-protein are associated through non-covalent interactions such that the native three-dimensional structure is largely similar and the active site geometry is practically identical to that of the native RNase A. It has been observed that the RNase A to RNase S conversion is not common to all the otherwise highly homologous ribonucleases of this class from different species. Pancreatic ribonuclease from kangaroo, reindeer, red deer, giraffe, dromedary and bovine could be cleaved with subtilisin at different positions between 18 and 21 in this external loop.[14,42] On the other hand, ribonucleases from rat, bovine seminal plasma, pig, coypu and lesser rorqual are not cleaved by subtilisin.[14,43] The three dimensional structure of bovine seminal RNase A which is a dimer has been determined.[9] This enzyme is not cleaved by subtilisin because the cleavage site is inaccessible due to the inter-monomer interactions in the dimer. Figure 1B lists the sequences of the loop 15–25 incorporating the subtilisin cleavage site for 11 different proteins of the ribonuclease A family including those of the rat and bovine enzymes. It is impossible to deduce sequence specificity from these sequences since the presence of proline, valine, tyrosine, and glutamic acid in the S-peptide loop does not interfere with the susceptibility to cleavage by subtilisin. Thus, subtilisin is considered a scavenger protease with a broad substrate specificity in terms of the amino acid sequences at which a protein can be cleaved.

The crystal structure of the recombinant rat RNase A indicates that the subtilisin resistance of rat RNase A can be explained on the basis of the conformation of the loop 15–25. This loop has a very different backbone conformation compared to that found in bovine ribonuclease A as seen from Figure 7. Figure 7A shows the electron density map for this loop which was independently rebuilt using OMIT maps. Figure 7B shows the superimposition of subtilisin cleavage site of rat and bovine RNase A. The loop 15–25 has relatively high temperature factors in the rat enzyme. The temperature factor values for this loop in the refined bovine structures are also higher than those for the rest of the protein. This may be due to the fact that the residues 19–21 form very few hydrogen bonds with the rest of the protein. Besides, the loop is exposed to solvent and is not involved in any crystal packing.

The side chain as well as backbone interactions involving the residues in the loop are critical in endowing

different conformations for the loop in the two enzymes. The main chain amide of 15T is hydrogen-bonded to main chain carbonyl of 17G in the rat enzyme. However, in the bovine enzyme, the corresponding amide of 15S is stabilized by hydrogen bonds to the symmetry related 23S and a water molecule. Residue 16 in bovine is stabilized by hydrogen bonds to residue 14, whereas, in the rat enzyme it is stabilized by the water molecules. Residue 18 in rat enzyme is a proline which is substituted by serine in bovine. Carbonyl O of 18P is hydrogen-bonded to amide N of 20K and Oγ of 21S. The counterpart interactions in the bovine enzyme are formed by hydrogen bonds between carbonyl O of 18S and Oγ of 80S and between N of 18S and a water molecule. The side chain Oγ of 18S is hydrogen-bonded to Oδ1 of symmetry related 24N. Q101 is responsible for stabilizing 20A in bovine, whereas, 101D stabilizes 21S in rat. The 23S in bovine is mutated to 23P in rat which is hydrogen-bonded to two water molecules.

The molecular docking of this region of the rat enzyme in the active site of subtilisin shows steric incompatibility suggesting conformational specificity associated with subtilisin activity. The computer docking of this loop, from both rat and bovine RNase A, into the active site of subtilisin was carried out using subtilisin-chymotrypsin inhibitor structure (pdb2sni) as a template. The bovine RNase A loop was first superimposed by least squares fit on the reactive site loop of chymotrypsin inhibitor in subtilisin-chymotrypsin inhibitor complex. Subsequently, the rat RNase A was also similarly superimposed on the bovine enzyme. The superimposition of the resulting molecular complexes of subtilisin with the two ribonucleases is shown in Figure 8. It is evident that the loop of the bovine RNase A fits into the active site without any steric constraints. On the other hand, the loop of the rat enzyme leads to a large number of short contacts. Thus, the resistant ribonucleases cannot adopt a conformation that can be accommodated in the active site of subtilisin. It is the presence of a particular type of structure in the bovine enzyme that leads to the pronounced proteolytic susceptibility of this region, whereas, absence of such a structure in rat enzyme confers it subtilisin resistant.

The site-specific cleavage by a protease is important in the post-translational processing of many proteins. Many examples have been illustrated where the site specificity is defined in terms of a sequence signature. Electrostatic effects have also been considered to be important for defining this specificity.[44,45] Steric effects have always been considered in order to provide basis for the specificity of any proteolytic enzyme towards its substrate. However, explicit correlation of the conformational restrictions arising in the substrate selection has not been demonstrated. Surface loops, the most divergent regions in homologous proteins, often play only a minor role in dictating protein structural stability. But their substitution can be of significance in protein-protein recognition processes. Thus, it is natural to expect that the loop 15–25 is likely to be cleaved most easily as it is the most exposed part of the intact RNase A. However, the results described above indicate that the rat RNase A is resistant to subtilisin due to the conformational features which do not allow suitable docking of the loop into the active site of the protease.

ACKNOWLEDGMENTS

This work was supported by the funds provided to the National Institute of Immunology by the Department of Biotechnology (Government of India). We thank Prof. M. Vijayan and Dr. K. Suguna for help during initial data collection and Dr. K. Kaur for critically reading the manuscript.

REFERENCES

1. Richards FM, Wyckoff HW. Bovine pancreatic ribonuclease. In: Boyer PD, editor. The enzymes, volume 4. New York: Academic Press; 1971. p 647–806.
2. Blackburn P, Moore S. Pancreatic ribonuclease. In: Boyer PD, editor. The enzymes, vol 15. New York: Academic Press; 1982. p 317–443.
3. Eftink MR, Biltonen RL. Pancreatic ribonuclease A: the most studied endoribonuclease. In: Neuberger A, Blocklerhurst K, Editors. Hydrolytic enzymes. Amsterdam: Elsevier; 1987. p 333–376.
4. Beintema JJ. Structure, properties and molecular evolution of pancreatic type ribonucleases. Life Chem Rep 1987;4:333–389.
5. D'Alessio G, Riordan JF, editors. Ribonucleases: structures and functions. New York: Academic Press; 1997. 670 p.
6. Kartha G, Bello J, Harker D. Tertiary structure of ribonuclease. Nature 1967;213:862–865.
7. Wyckoff HW, Tsernoglou D, Hanson AW, Knox JR, Lee B, Richards FM. The three-dimensional structure of ribonuclease-S. J Biol Chem 1970;245:305–328.
8. Carlisle CH, Palmer RA, Mazumdar SK, Gorinsky BA, Yeates DGR. The structure of ribonuclease at 2.5 Å resolution. J Mol Biol 1974;85:1–18.
9. Mazzarella L, Capasso S, Demasi D, Di Lorenzo G, Mattia CA, Zagari A. Bovine seminal ribonuclease: Structure at 1.9 Å resolution. Acta Crystallogr D 1993; 49:389–402.
10. Acharya KR, Shapiro R, Allen SC, Riordan JF, Vallee BL. Crystal structure of human angiogenin reveals the structural basis for its functional divergence from ribonuclease. Proc Natl Acad Sci USA 1994;91:2915–2919.
11. Mosimann SC, Ardelt W, James MNG. Refined 1.7 Å X-ray crystallographic structure of P-30 protein, an amphibian ribonuclease with anti-tumor activity. J Mol Biol 1994;236:1141–1153.
12. Varadarajan R, Richards FM. Crystallographic structures of ribonuclease S variants with nonpolar substitution at position 13: packing and cavities. Biochemistry 1992;31:12315–12327.
13. Varadarajan R, Connelly PR, Sturtevant JM, Richards FM. Heat capacity changes for protein peptide interactions in the ribonuclease S system. Biochemistry 1992;31:1421–1426.
14. Welling GW, Groen G, Gabel D, Gaastra W, Beintema JJ. The preparation and primary structure of S-peptides from different pancreatic ribonucleases. FEBS Lett 1974;40:134–138.
15. Sambrook J, Fritsch EF, Maniatis T, editors. Molecular cloning: a laboratory manual. Cold Spring Harbor, NY: Cold Spring Harbor Laboratory; 1989. 1379 p.
16. Stanssens P, Opsomer C, Mckeown YM, Kramer W, Zabeau M, Fritz H-J. Efficient oligonucleotide-directed construction of mutations in expression vectors by the gapped duplex DNA method using alternating selectable markers. Nucleic Acids Res 1989;17: 4441–4454.
17. Neu H, Heppel L. The release of enzymes from *Escherichia coli* by osmotic shock and during the formation of spheroplasts. J Biol Chem 1965;240:3685–3692.
18. Crook EM, Mathias AP, Rabin BR. Spectrophotometric assay of bovine pancreatic ribonuclease by the use of cytidine 2′:3′-phosphate. Biochem J 1960;74:234–238.
19. Otwinowski Z. DENZO. In: Sawyer L, Issacs N, Bailey S, editors. Proceedings of the CCP4 study weekend: data collection and processing. Daresbury, England: SERC Daresbury Laboratory; 1993. p 56–62.
20. Navaza J. AMoRE: an automated package for molecular replacement. Acta Crystallogr A 1994;50:157–163.

21. Wlodawer A, Svensson LA, Sjölin L, Gilliland GL. Structure of phosphate free ribonuclease A refined at 1.26 Å. Biochemistry 1988;27:2705–2717.
22. Bernstein FC, Koetzle TF, Williams GJB, et al. The protein data bank: a computer-based archival file for macromolecular structures. J Mol Biol 1977;112:535–542.
23. Brünger AT. XPLOR version 3.1: a system for X-ray crystallography and NMR. New Haven;Yale University Press;1992. 382 p.
24. Jones TA, Cowan S, Zou JY, Kjeldgaard M. Improved methods for building protein models in electron density maps and the location of errors in these models. Acta Crystallogr A 1991;47:110–119.
25. Beintema JJ, Schüller C, Irie M, Carsana A. Molecular evolution of the ribonuclease superfamily. Prog Biophys Mol Biol 1988;51:65–192.
26. Heijne VG. A new method for predicting signal sequence cleavage sites. Nucleic Acids Res 1986;14:4683–4690.
27. Beintema JJ, Campagne RN, Gruber M. Rat pancreatic ribonuclease: isolation and properties. Biochim Biophys Acta 1973;310:148–160.
28. Tartof KD, Hobbs CA. Improved media for growing plasmid and cosmid clones. Bethesda Res Lab Focus 1987;9:12.
29. Matthews BW. Solvent content of protein crystals. J Mol Biol 1968;33:491–497.
30. Luzatti P.V. Traitment statistique des erreurs dans la détermination des structures crystallines. Acta Crystallogr 1952;5:802–810.
31. Richards FM, Wyckoff HW. Ribonuclease-S. In: Phillips DC, Richards FM, editors. Atlas of molecular structures in biology, vol. 1. Oxford: Oxford University Press (Clarendon); 1973. p 1–75.
32. Cuchillo MC, Vilanova M, Nogués MV. Pancreatic ribonucleases. In: D'Alessio G, Riordan JF, editors. Ribonucleases: structures and functions. New York: Academic Press; 1997. p 271–304.
33. Borkakoti N, Moss DS, Palmer RA. Ribonuclease-A: least-squares refinement of the structure at 1.45 Å resolution. Acta Crystallogr B 1982;38:2210–2217.
34. Wlodawer A, Miller M, Sjölin L. Active site of RNase: neutron diffraction study of a complex with uridine vanadate, a transition-state analog. Proc Natl Acad Sci USA 1983;80:3628–3631.
35. Martin PD, Doscher MS, Edwards BFP. The refined crystal structure of a fully active semisynthetic ribonuclease at 1.8-Å resolution. J Biol Chem 1987;262:15930–15938.
36. Nachman J, Miller M, Gilliland GL, Carty R, Pincus M, Wlodawer A. Crystal structure of two covalent nucleoside derivatives of ribonuclease A. Biochemistry 1990;29:928–937.
37. deMel VSJ, Martin PD, Doscher MS, Edwards BFP. Structural changes that accompany the reduced catalytic efficiency of two semisynthetic ribonuclease analogs. J Biol Chem 1997;267:247–256.
38. Borkakoti N, Palmer RA, Haneef I, Moss DS. Specificity of pancreatic ribonuclease-A: an X-ray study of a protein-nucleotide complex. J Mol Biol 1983;169:743–755.
39. Wlodawer A, Sjölin L. Structure of ribonuclease A: results of joint neutron and X-ray refinement at 2.0 Å resolution. Biochemistry 1983;22:2720–2728.
40. Lisgarten JN, Gupta V, Maes D, et al. Structure of the crystalline complex of cytidylic Acid (2′-CMP) with ribonuclease at 1.6 Å resolution. Conservation of solvent sites in RNase A high-resolution structures. Acta Crystallogr D 1993; 49:541–547.
41. Richards FM,Vithayathil PJ. The preparation of subtilisin-modified ribonuclease and the separation of the peptide and protein components. J Biol Chem 1959;234:1459–1465.
42. Oosterhuis S, Welling GW, Gaastra W, Beintema JJ. Reinvestigation of the primary structures of red deer and roe deer pancreatic ribonuclease and proline sites in mammalian ribonucleases. Biochim Biophys Acta 1977;490:523–529.
43. Parente A, Branno M, Malorni MC, Welling GW, Libonati M, D'Alessio G. Proteolytic enzymes as structural probes for ribonuclease BS-1. Biochim Biophys Acta 1976;445:377–385.
44. Wells JA, Powers DB, Bott RR, Graycar TP, Estell DA. Designing substrate specificity by protein engineering of electrostatic interactions. Proc Natl Acad Sci USA 1987;84:1219–1223.
45. Ballinger MD, Tom J, Wells JA. Designing subtilisin BPN' to cleave substrates containing dibasic residues. Biochemistry 1995; 34:13312–13319.